Neuromorphic Analog VLSI Sensors for 2-D Direction of Motion

Rainer A. Deutschmann[1,2], Charles M. Higgins[2] and Christof Koch[2]

[1] Technische Universität, München
[2] California Institute of Technology
Pasadena, CA 91125
rainer@klab.caltech.edu

Abstract. Optical flow fields are a primary source of information about the visual scene in technical and biological systems. In a step towards a system for real time scene analysis we have developed two new algorithms for the parallel computation of the direction of motion field in 2-D. We have successfully implemented these algorithms in analog VLSI hardware such that all processing is performed in the focal plane of the imager. We present data from 12×13 and 15×14 test arrays and show that the sensors are reliable for over one order of magnitude in velocity and down to 20% contrast. The algorithms allow for a very small pixel size ($110\mu m \times 110\mu m$ in a $1.2\mu m$ CMOS process) and thus high resolution arrays are feasible.

1 Introduction

Moving scenes are a rich source of information. From the optical flow important parameters such as ego-motion, time-to-contact and the focus of expansion can be inferred. Object segmentation and figure-ground segmentation based on edge detection can be improved by using discontinuities of the optical flow field.

The analysis of moving scenes has commonly been performed on serial computer systems, where the computation of the optical flow field above video rate is rarely achieved and the required computing power increases drastically for higher resolutions. In contrast, biological systems from insects to humans can operate in real time due to the parallel processing of the optical information. In particular in primates area MT is the first visual area where neurons respond selectively to velocity over a wide range of spatial frequencies. In area V1, which directly projects to MT, cells with reliable selectivity for only direction of motion are found. Additionally, these cells also can only report the component of motion perpendicular to an oriented edge.

Encouraged by the fact that there are cells in primate V1 that respond to direction of motion we have developed and implemented two new algorithms for the computation of the local direction of motion of a 2-D moving scene. Since the computation of the direction of motion requires much less sophisticated implementations than the computation of the local velocity we were able to achieve a very small cell size. This in turn is a necessary requirement for building biologically inspired high-level vision systems where for visual information integration at least several hundred cells are required. We are now equipped with highly integrated sensors that compute high resolution flow fields in real time. The sensors are similar to biological systems in that they operate in parallel and in real time, they code signals in graded potentials as well as in spikes, they are power efficient and are adaptive to different lighting conditions. The sensors only require nearest neighbor interaction and use design principles proven to be very robust in previous implementations of 1-D velocity sensors [Kra96],[KSK97].

2 Direction of Motion Algorithms

Both sensors use the occurrence of an intensity edge at neighboring pixels as an indicator for its direction of motion. An intensity edge is detected with a temporal edge detector (TED) [KSK97], a nonlinear feedback circuit. A thresholding amplifier generates a voltage spike when a large enough

temporal intensity change has occured. The voltage spike is fed into the direction of motion circuits, which we describe in sections 2.1 and 2.2 for the 1-D case. Two 1-D direction of motion units per pixel are combined for the 2-D sensor. Each pixel in the array reports the direction of motion in two tri-state currents (positive, zero and negative) representing the X and Y direction. A total of 9 different output combinations is therefore possible, 8 of which indicate the direction of motion in 2-D in steps of 45 degrees, the ninth indicating zero motion. The output currents persist for an adjustable time τ_{pt} after initiation before resetting themselves to zero.

2.1 Facilitate, Trigger and Compare (FTC) Algorithm

When an edge crosses any pixel, locally a facilitation time window is opened. The pixel is now sensitive to receiving a spike signal from any neighbor. As the edge moves on, it will eventually cross a neighboring pixel and initiate a spike. Within the facilitation period τ_{fac} this spike from a neighboring pixel can trigger the direction of motion indicator. Which of the two opposing directions has been triggered determines the sign of the local output current. This current lasts for τ_{pt} (see Figure 1).

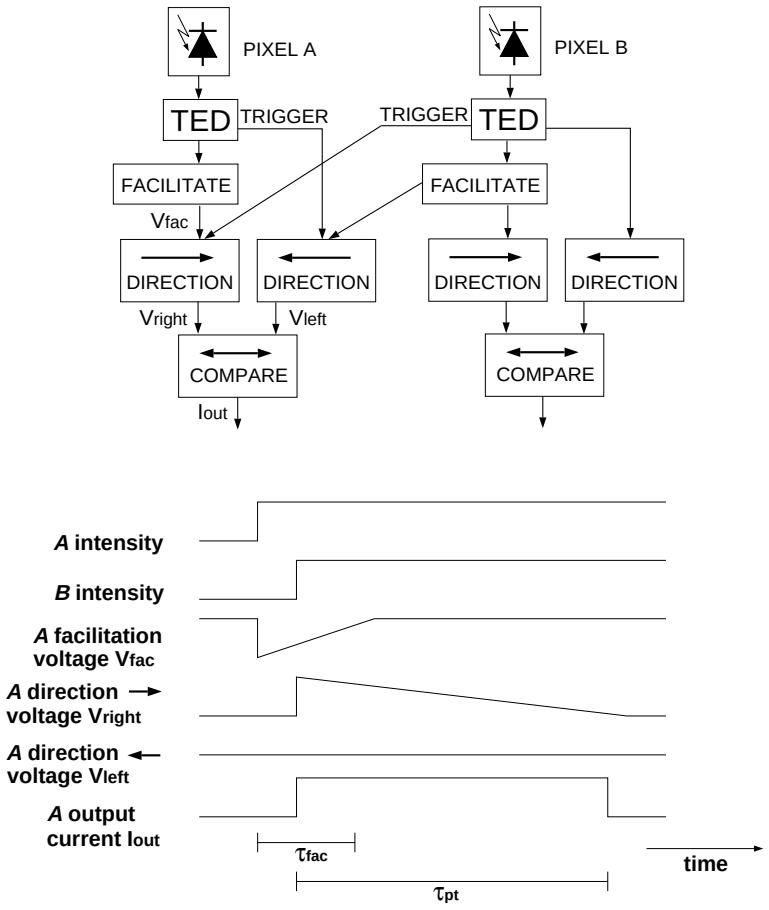

Fig. 1. FTC sensor, 1-D block diagram and signal flow: For an edge moving from left to right, first pixel A is facilitated and the voltage V_{fac} goes low. As the edge crosses pixel B, in pixel A the rightward motion indicator is triggered with voltage V_{right} going high. V_{right} >0 and V_{left} =0 in pixel A are compared and a positive output current is generated indicating that the edge moved to the right. The null-direction output is suppressed because pixel B has not been facilitated before the leftward motion indicator in pixel A is triggered.

2.2 Inhibit-Trigger-Inhibit (ITI) Algorithm

In the ITI algorithm a TED spike due to a moving edge triggers the indicator for both directions with the voltages V_{left} and V_{right} going high. The neighboring pixel which is next crossed by the edge then inhibits the null-direction output, either V_{left} or V_{right} is reset to zero. The direction of motion output is computed as the difference of the two opposing direction indicators (see Figure 2).

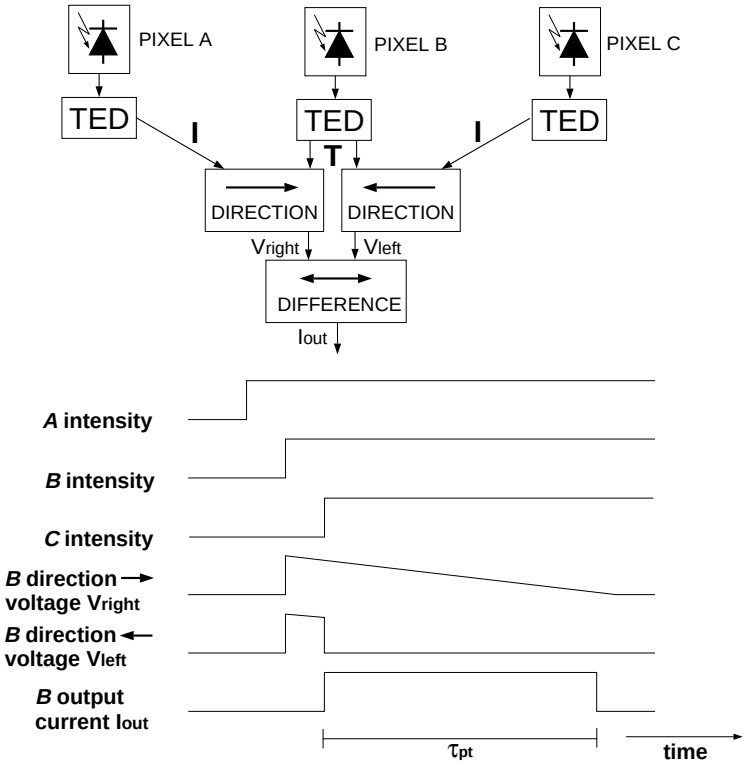

Fig. 2. ITI sensor: As pixel B is crossed by an edge moving from left to right, both V_{right} and V_{left} are triggered, but no output is reported because the difference is zero. As the edge passes pixel C, V_{left} is reset to zero and a positive current output indicating rightward motion is generated. Pixels B and A interact similarly to detect an edge moving left, producing a negative current output.

3 Results

Both sensors were implemented in a standard $1.2\mu m$ analog CMOS process on chips of the physical size 2.2×2.2mm. We achieved pixel sizes of $128\mu m \times 119\mu m$ (FTC) and $105\mu m \times 115\mu m$ (ITI) which allowed for a 12×13 and 15×14 pixel array, respectively. The output currents are read off the chip with serial scanners and are displayed on a Pentium PC. We easily achieve video frame rates and are limited by how fast the computer can handle the data. The real time performance will be maintained even for sensors with higher resolution because of their parallel architecture. On the next larger available chip size (4.6×4.7mm) arrays with resolutions of 32×32 could easily be achieved.

In sections 3.1 and 3.2 we characterize the performance of the elementary motion detectors over the whole array. In section 3.3 we show sample snapshots of the output of the FTC sensor.

3.1 Orientation Tuning Curve

We measured the elementary motion detector response by moving a full-field square wave grating stimulus over the sensor. We varied the stimulus angle while leaving the velocity and contrast of the stimulus constant and recorded the X and Y component of the local direction of motion vector. For very small photoreceptors and an optimal TED we expect the sensors to separate the two dimensional velocity space into four quadrants, for example the Y+ output would respond with a probability of one for stimulus angles from 0 to 180 degrees. The FTC sensor performs very much like this (see Figure 3 left). Due to the finite size of the photoreceptors, the finite pulse length and the probabilistic nature of the TED (not every edge presentation evokes a spike) the velocity space is in fact separated into 8 directions such that for example Y+ responds with a probability less than one for stimulus angles close to 0 or 180 degrees. This is most visible for the ITI sensor (see Figure 3 right and Figure 4).

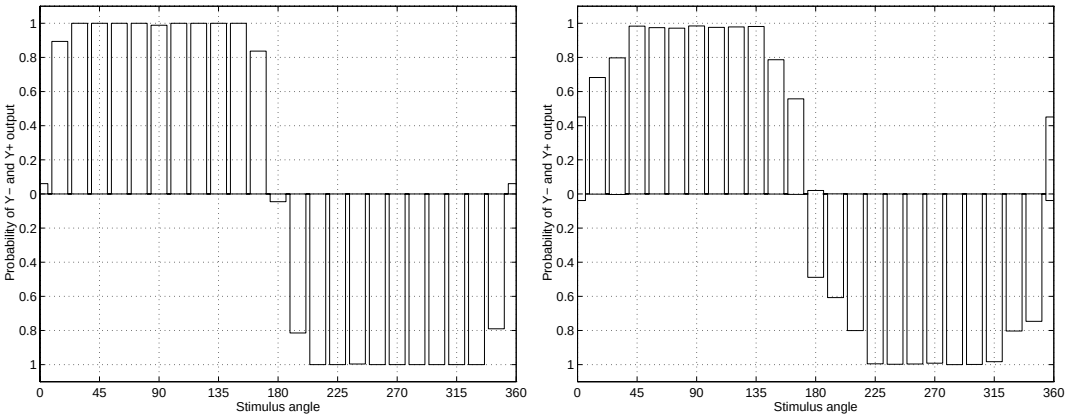

Fig. 3. Probability of Y+ output (top) and Y- output (bottom) for different stimulus angles shown for the FTC sensor (left) and the ITI sensor (right). Both sensors separate the velocity space reliably into four quadrants.

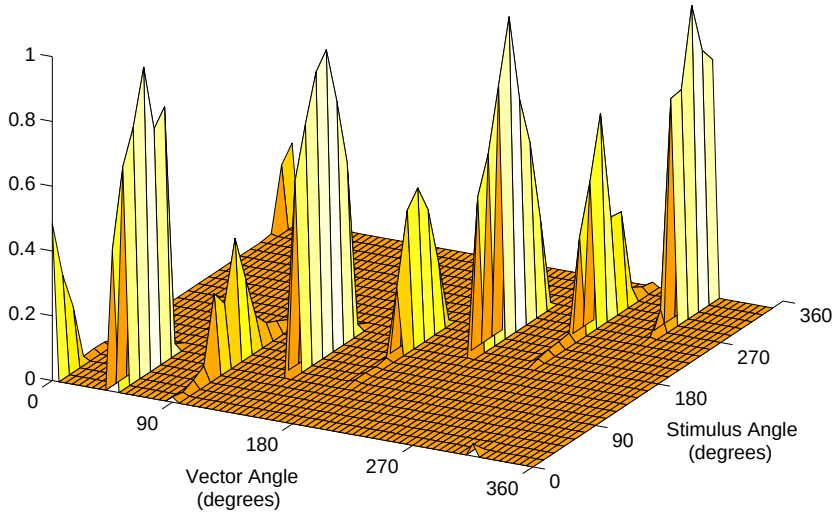

Fig. 4. Orientation response of the ITI sensor: Normalized histogram of the response vector angles as the stimulus angle is varied. As expected the reported vector angles vary with the stimulus angle in steps of 45 degrees. Note that there are only 8 possible output directions for a single vector, and that a diagonal response is more probable that a non-diagonal. The FTC chip has an even stronger tendency to respond with diagonal vectors than shown in the plot.

3.2 Velocity and Contrast Range

We measured the velocity and contrast ranges over which the correct direction of motion is reported. The sensors are capable of detecting both dark-to-bright and bright-to-dark edges. We present data obtained for bright to dark edges of different contrasts and velocities (see Figure 5). The sensor output was recorded simultaneously for the whole array over multiple stimulus presentations. The output was counted as correct if the reported vector direction was within $\pm$ 22.5 degrees of the stimulus direction. The FTC sensor was able to report the correct direction of motion with a confidence of 90% for stimulus velocities as low as we could generate them (<25 pixels/s) and as high as 450 pixels/s for contrasts above 40%. This velocity range of over one order of magnitude spans most of the biologically relevant velocities. For high contrasts the performance is 100%. The sensor was able to respond to contrasts as low as 10%.

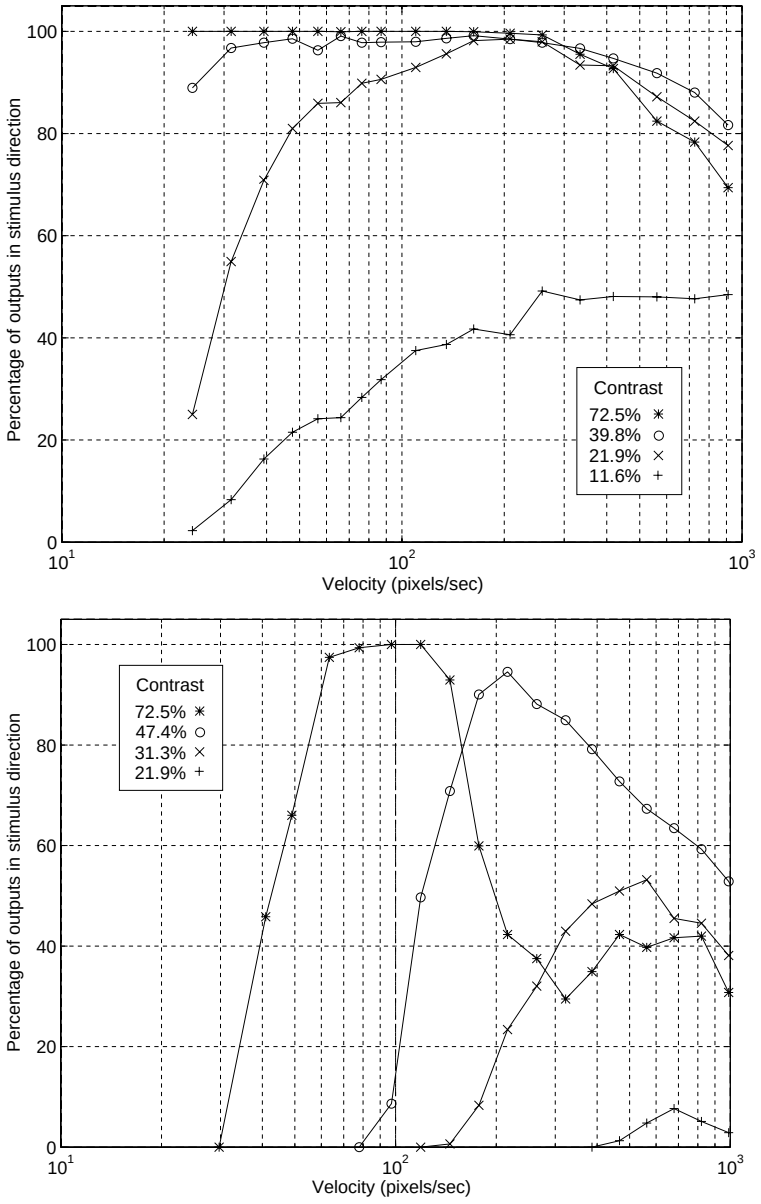

Fig. 5. Correct direction of motion output for the FTC sensor (top plot) and the ITI sensor (bottom plot). Due to a larger layout of the photoreceptor and TED the FTC sensor has a wider range of operation in velocity and contrast.

3.3 Flow Field Examples

In order to demonstrate the usefulness of the direction of motion flow fields, we present snapshots from the output of the FTC sensor in Figures 6 and 7.

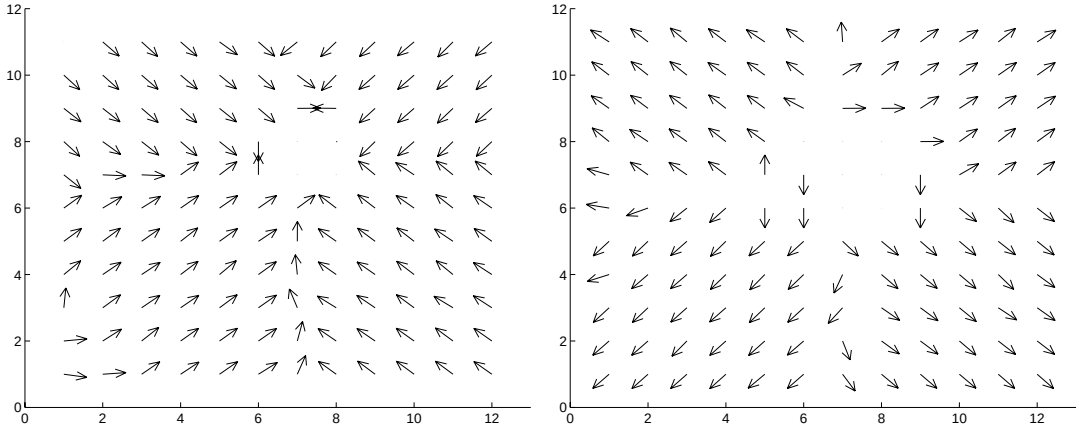

Fig. 6. Snapshots from the FTC sensor. The left field was obtained by moving a circular object away from the sensor. In the right field the object is approaching the sensor. The focus of expansion is obvious.

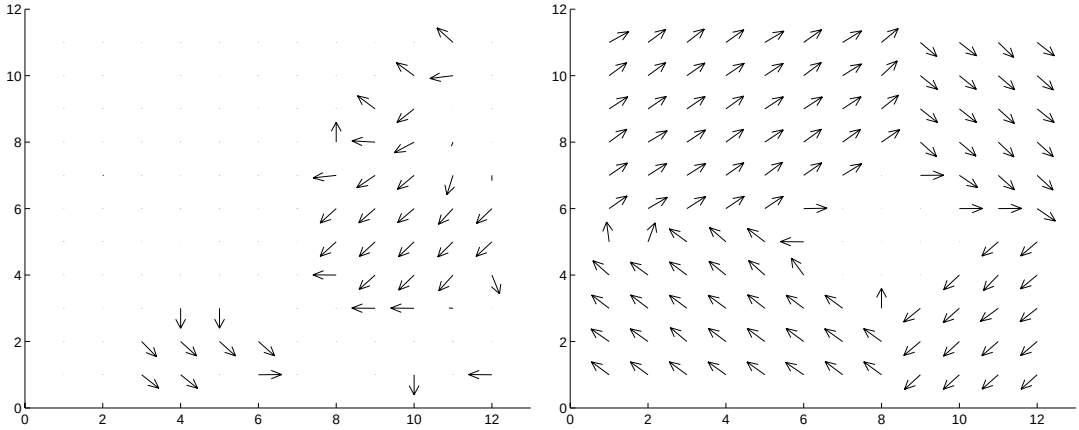

Fig. 7. In the left snapshot a small object moves down and to the right. At the same time a larger object is entering from the upper right corner. Segmentation from motion can be performed. The right flow field is the result for a wagon wheel pattern rotating over the sensor. Determination of the direction and axis of rotation is possible.

Acknowledgments RD was supported by the German National Merit Foundation. This work was supported by the Center for Neuromorphic Systems Engineering as a part of the National Science Foundation's Engineering Research Center program.

4 Bibliography

References

[Kra96] J. Kramer. Compact integrated motion sensor with three-pixel interaction. *IEEE Trans. Pattern Anal. Machine Intell*, 18:455–560, 1996.

[KSK97] J. Kramer, R. Sarpeshkar, and C. Koch. Pulse-based analog VLSI velocity sensors. *IEEE Trans. Circuits and Systems II*, 44:86–101, 1997.